京都大学防災研究所年報 第 49 号 B 平成 18 年 4 月
Annuals of Disas. Prev. Res. Inst., Kyoto Univ., No. 49 B, 2006

Conjunctive Simulation of Surface and Subsurface Flow within Water Budget

Sina NASOUHI*, Toshio HAMAGUCHI and Toshiharu KOJIRI

* Graduate School of Engineering, Kyoto University

Synopsis

Conjunctive use of surface and ground water resources can prevent "aquifer mining" by imposing upper and lower lumped operation rules on the net withdrawal, through analyzing long time inflow to the system. To achieve this, mathematical developments were proposed that involve piston flow equations into more natural initial and boundary conditions. This facilitates considering a two-piston coupling mechanism between kinematic wave model and an analytical water budget model for recharge. The proposed methodology was verified for soil columns, and finally applied to typical arid region condition.

Keywords: Conjunctive use, Operation rules, Piston flow, kinematic wave, analytical water budget, ground water recharge, perturbation theory

1. Introduction

Traditionally, deriving "operation rules" for multi-reservoirs by modelists, provide convenient tools for "decision makers" without involving them into the detailed modeling procedure. Nevertheless when it comes to "conjunctive use of surface and ground water resources", they have to face to complex hydrological models at regional scale, or too simplified optimization models at basin scale. It is due to this confliction that while driving operation rules is based on application of reservoir models for long-time historical data, the essential environmental impacts need to be simulated through distributed system. This is more significant in arid to semi-arid regions where considering additional dams are not feasible and large aquifers make important water resources of the area. Under such conditions, intensive well pumping more than "sustainable yield" of aquifers results in "aquifer mining" and infra-structure damage due to the land settlement. Also, improper irrigation practice not only may results in soil salinity and crop yield reduction, but also may degrade groundwater quality below the consumption standards by introducing agrochemical pollutants. Although many conjunctive-use studies have considered some of these impacts separately, still integrating them in such a way that can provides practical charts and rules for "decision makers", remains as a challenging task.

The mere aim of this study is to fill out this gap by integrating effective hydrological processes and environmental impacts, and providing sensible "operation rules" for decision makers. Though at the first step and for the sake of simplicity this report just considers "aquifer mining", and try to propose some basic rules by means of simultaneous (conjunctive) simulation of surface and subsurface flow within a distributed system controlled by a water budget model.

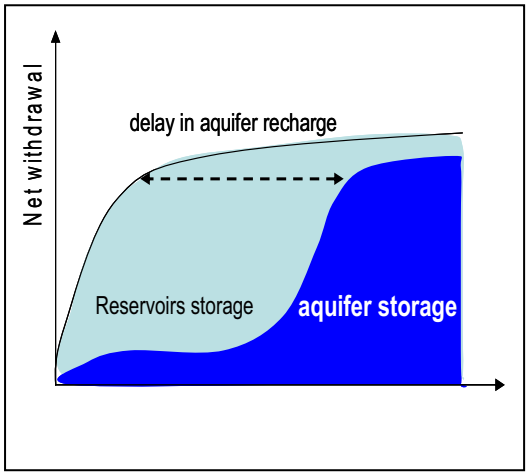

Fig. 1 effect of lag time in recharge on allocation of the net withdrawal

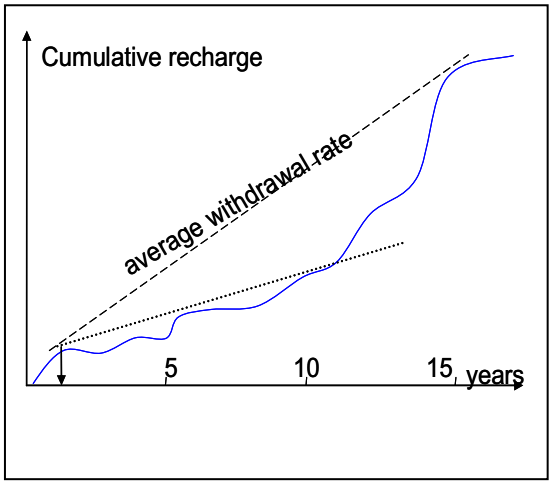

Fig. 2 mass curve analysis of long time aquifer recharge

2. Methodology

As a practical methodology, first some basic operation rules are proposed, and then the required modeling approach will be discussed.

2.1 Basic operation rules

Defining lumped operation rules as the weighted average of the reservoirs release and net withdrawal from aquifers, then such weighting factors would be affected chiefly by lag time in inflow to the aquifer (recharge). Schematically it can be shown in Fig.1 where reservoir release is in priority due to the short travel time of run-off. Because of variable depth of water table this lag time in recharge needs to be simulated through distributed system.

Note that the storage terms in Fig.1 are dynamic or "renewable" ones. Traditionally, these terms can be estimated by "mass curve analysis" of historical inflow into the reservoirs. Now, considering each ground water model cell as a reservoir, then once we achieve simulating long time subsurface inflow to the aquifer (recharge) at each cell, then the some technique can be expanded to estimate renewable storage. It implies temporal and spatial distribution of "safe yield", which in turn imposes upper and lower constraints on the net discharge.

2.1.1 Lumped upper rules

The net withdrawal should not exceed the maximum probable recharge events in a period of 15 to 20 years ahead (see section 6.5 for more discussion). An example for such permissible withdrawal (demand) rate has been marked by the dashed line in Fig.2. In other words, assuming water table depth at minimum recharge condition, the marked average demand rate may results in temporary decrease in ground water level for a few years but eventually it should be compensated by the large recharge event at the end of each renewable period.

2.1.2 Lumped Lower rules

The minimum net withdrawal from storage is needed to provide enough room for the maximum probable recharge event so that it minimizes water table evapotranspiration, seepage and over flow from aquifer into low quality water bodies. For example withdrawal rate marked by dotted line in Fig.2 can not be an effective policy when the water table depth is at average condition, and the maximum recharge exceeds the effective aquifer storage.

2.1.3 Primitive allocation rules

Once the lumped permissible withdrawal within each period is obtained, in the next step the spatial allocation of these net values from different ground water model cells (well fields) can be weighted by aerial recharge and net lateral inflow to each model cell. Yet, due to the difficulty in estimation of the aerial recharge components, this report focuses on generating of historical recharge in different model cells as "primary allocation coefficients" (see 6.5 for more discussion).

Table 1 different hydrologic conditions at conjunctive use domain

	Mountainous river basin area	Flatter plain and field area
hydro-geologic setting	- thin soil layers including local subsurface storages linked to the rivers - rivers are mainly "gaining" type	- think deposits including large aquifers at higher depth - rivers are mainly "loosing" type
dominant hydrologic process	- saturation excess overland flow - lateral subsurface flow to river (through flow, interflow, base flow)	- infiltration excess (Hortonian) overland flow - vertical percolation to the aquifers
convenient governing equations	- kinematic wave for main direction on steeper slope - linear reservoir equations for simultaneous horizontal and vertical subsurface flow	- kinematic wave overland flow over low slope in all directions -1D Richard equation for vertical percolation.

2.2 Modeling approach

Regarding the proposed operation rules, the essential hydrologic processes that need to be simulated can be decided. Further, considering important initial and boundary condition for conjunctive use will provide the clue toward the required mathematical development in the following section.

2.2.1 Choice of the governing equations

The proposed basic operation rules require a model that simulates long-time surface-subsurface inflow through a distributed system. It implies a fast model which can consider the dominant hydrological processes as well. Though, due to the regional scale of conjunctive use, these dominant processes can be different in the mountainous river basin area, and the flatter plain area overlying on aquifers (Table 1). Note that in the former sub-area subsurface serial linear storage model provides a more feasible estimation of simultaneous lateral and vertical subsurface flow compared to two or three dimensional Richard equation (see section 6.1). In practice, while "conjunctive use studies" cover both areas, the "conjunctive use management" happens in plain area where ground water storages are being enough to be considered as aquifers. In such condition due to gentle slope and large ratio of the area to the depth of water table, the horizontal component of subsurface flow is ignorable and one dimensional Richard equation can estimate flow with acceptable accuracy.

2.2.2 Method of solution

Recalling the essence of a fast calculation procedure which can integrate dominant hydrological processes, numerical solutions of kinematic wave model are quite convenient. Though common numerical solutions of Richard equation which ignore "random field of unsaturated hydraulic conductivity" for each type of soil, can lead to significant error in runoff and recharge components over regional scales (Sharma et al, 1979).

Traditionally two approaches have been proposed to overcome this problem. The first one is based on "linearization" of Richard equation around "effective hydraulic conductivity" by forcing the resultant small perturbation to zero values. This technique is most suitable for smaller scale area where the ratio of area to depth of soil is not large. In addition, its numerical frame work makes it too slow for applications like this research that need numerous model run. The other method is based on simplifying Richard equation by "delta function technique" that results in analytical solutions such as Green-Ampt model for infiltration, or in more general sense "piston flow" equations.

Dagan and Bresler (1981) were the first who could generalize piston flow equations through the entire infiltration-redistribution cycle for an assumed homogenous soil column. Then, considering a single "heterogeneous" model cell as a population of "Parallel Homogeneous Columns" (PHC) with lognormal distribution around the assumed permeability value, they utilized a Monte-Carlos simulation scheme for averaging

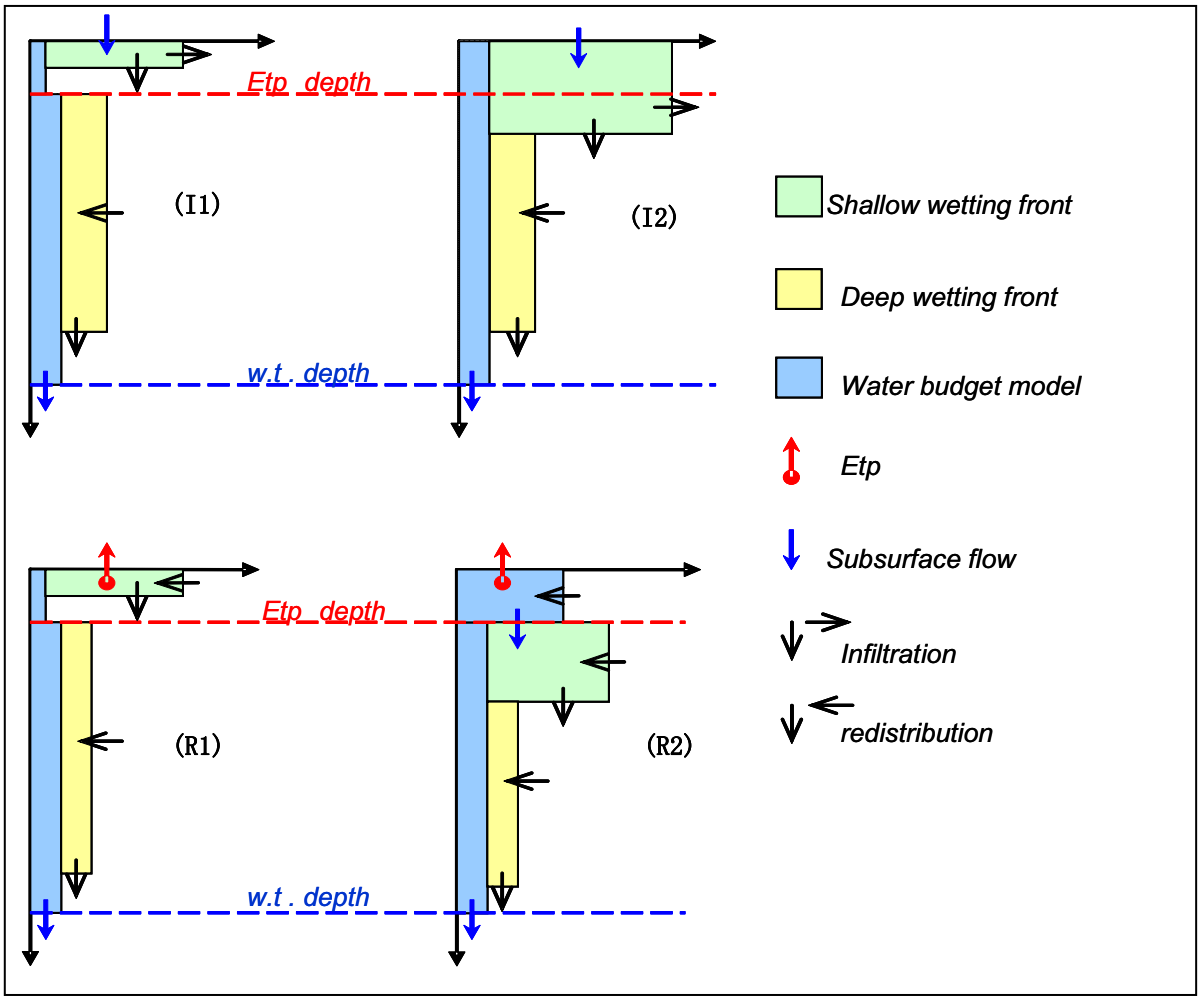

Fig. 3 Initial and boundary conditions at early (1) and late (2) stage of infiltration (I) and redistribution (R). (See section 4.2 for more details)

flow over the entire cell. They could show that the estimation error of their analytical solution is canceled out over a heterogeneous field and can provide more reliable solution compared to deterministic numerical models. Nevertheless, their piston flow equations were limited in terms of handling some of important natural initial and boundary conditions that are common at conjunctive use applications. Consequently, common Conjunctive-use studies still use deterministic numerical approach which can be prone to high error at regional scale, and too slow to generate long recharge time series.

2.2.3 Initial and boundary conditions

To handle more practical boundary and initial conditions, this study reformulates a "two-piston flow" coupling mechanism within an analytical water budget model, which facilitates simultaneous (conjunctive) simulation of long-term surface and subsurface inflow to the underlying aquifer (Fig.3). The choice of two-piston flow mechanism has been based to this fact that assumption of instantaneous distribution of rainfall through all the soil profile may lead to significant error in delay time for deep water table condition. On the other hand, driving wetting fronts for each set of boundary conditions (storm events) results in several parallel pistons which for long time record of storm events can be confusing. However even such simplification imposes different boundary and initial conditions. Table 2 summarizes these new important conditions and the required mathematical development regarding initial and boundary condition in Fig.3.

Table 2 Mathematical development for more realistic initial and boundary conditions

	Initial and boundary condition	Mathematical development
Infiltration period	1D kinematic wave in all directions	Implicit reformulation of isoparametric kinematic wave model
	Continuous infiltration over both plain and mountainous (with interflow) area	Equivalent series for piston flow equation
	Effect of surface soil moisture deficiency on runoff pounding time	Switching between initial moisture profiles
	Variable rainfall before runoff	Infiltration phase under variable flux boundary
Redistribution period	Simultaneous soil evapotranspiration and percolation (R1)	Redistribution under soil evapotranspiration
	Leakage from upper root zone (R2)	Redistribution under flux boundary condition

3. Mathematical development

3.1 Equivalent series solution for piston flow

For real soils, the governing equation for one-dimensional flow, equation (1), results in the well-known Philip (1957) time series and cumulative infiltration (*F*).

$$\frac{\partial \theta}{\partial t} = \frac{\partial}{\partial z}\left[K(\theta)\frac{\partial \psi}{\partial \theta}\frac{\partial \theta}{\partial z} - K(\theta) \right] \quad (1)$$

$$z(\theta,t) = A_1(\theta)t^{1/2} + A_2(\theta)t\ A_3(\theta)t^{3/2} + \Lambda \quad (2)$$

$$F = S_p t^{\frac{1}{2}} + C_a t \qquad t \le t_{grav} = \left(\frac{S_p}{K_s - K(s_n)} \right)^2 \quad (3)$$

Where A_n are solutions of ordinary differential equations; and t_{grav} is experimental convergence criteria (characteristic time) in terms of Sorptivity (S_p), initial saturation (S_n) and hydraulic conductivity (K). For delta function soils under ponded infiltration, the governing equation reduces to equation (4) with the implicit solution as equation (5).

$$\frac{dL}{dt} = \mu . K_s \left(1 + \frac{\alpha}{L} \right) \quad (4)$$

$$\frac{tK_s\mu}{\alpha} = \frac{L(t)}{\alpha} - Ln\left[1 + \frac{L(t)}{\alpha} \right] \quad (5)$$

Where

$$\alpha = \frac{[\phi(1) - \phi(s_n)]}{1 - K_r(s_n)} \ , \ \mu = \frac{1 - K_r(s_n)}{n_e(1 - s_n)} \quad (6)$$

$$s = \left(\frac{\psi_b}{\psi} \right)^{\lambda} \quad , \quad K_r = \frac{K(\theta)}{K_s} = s^{\eta/\lambda} \quad (7)$$

$$\phi_r(s) - \int K_r(s)\frac{d\psi}{ds} d_s = \frac{\psi_b}{1-\eta} s^{\eta - 1/\lambda} \quad (8)$$

Here ϕ(s) is Gardner flux potential which was used by Chen et al (1994) to obtain a simpler form of Dagan-Bresler equations. To obtain an explicit form of equation (5), many authors have expanded the logarithm term and thus calculated Philip equation parameters by analogy with equation (2). Yet, the validation of equivalent Philip's t_{grav} concept for delta-function soils (piston profile) remains under doubt. Although Later Salvucci and Entekhabi (1994) proposed a convergent series for approximation of equation (5); none of these approaches are direct solutions of the governing equation (4) and thus can't discuss directly the domain where they approximate it: a task we are doing here by utilizing perturbation theory.

3.1.1 Perturbation theory

Due to the perturbation theory, considering a group of similar equations, then the solution of a difficult one can be stated in terms of a simple one through a series of parameter λ ; which tends to unity (Courant and Hilbert, 1989). Accordingly, rewriting of equation.(4) in terms of λ (equation (8)), suggests a simple (unperturbed) differential equation (equation.(9)), with an exact solution.

$$L\frac{dL}{dt} = \mu\lambda + \alpha\lambda \qquad \lambda = \mu K_s \tag{8}$$

$$L_0\frac{dL_0}{dt} = \mu\lambda \qquad L_0(t) = \sqrt{2\alpha\lambda t} \tag{9}$$

Hence, by considering equation (8) as a perturbed form of equation (9), an approximate solution can be sought according to perturbation theory.

$$L(t) = a_0 + \lambda a_1 + \lambda^2 a_2 + \Lambda + \lambda^n a_n \tag{10}$$

$$a_n = a(t) \ , \ a_0 = L_0(t) \tag{11}$$

Substituting of equation (10) into equation (8) and differentiating refer to time results in:

$$\begin{aligned}&(a_0 + \lambda a_1 + \lambda^2 a_2 + \Lambda)(a_0' + \lambda a_1' + \lambda^2 a_2' + \Lambda) \\ &= \lambda(a_0 + \lambda a_1 + \lambda^2 a_2 + \Lambda) + \lambda K_s\end{aligned} \tag{12}$$

Where a_n' are time derivative. Now, expanding of the left and right hand side of equation (12) and re-arranging in terms of λ^n leads to the following equations

$$LHS \therefore \quad a_0 a_0' + [a_0' a_1 + a_0 a_1']\lambda + [a_0' a_2 + a_1 a_1' + a_2 a_0']\lambda^2 + \Lambda \tag{13}$$

$$RHS \therefore a_0\lambda + a_1\lambda^2 + \Lambda + \lambda K_s \tag{14}$$

By equating corresponding coefficient of λ^n in equation (13) and (14); and after simplification, a set of ordinary differential equations are obtained as below

$$n = 0 \therefore a_0 a_0 = \lambda K_s + C_0 \Rightarrow a_0 = \sqrt{2\lambda K_s} + C_0 \tag{15}$$

$$n = 1 \therefore (a_0 a_1)' = a_0 \Rightarrow a_1 = \frac{1}{a_0}\left[\int a_0 dt\right] + \frac{C_1}{a_0} \tag{16}$$

$$n = 2 \therefore (a_0 a_2)' = a_1 - a_1 a_1)' \Rightarrow a_2 = \frac{1}{a_0}\left[\int a_1 dt\right] + \frac{C_2}{a_0} \tag{17}$$

$$\begin{aligned}&n = 3 \therefore (a_0 a_3)' = a_2 - (a_1 a_2)' \\ &\Rightarrow a_3 = \frac{1}{a_0}\left[\int a_2 dt - a_1 a_2\right] + \frac{C_3}{a_0}\end{aligned} \tag{18}$$

$$\begin{aligned}&n = 4 \therefore (a_0 a_4)' = a_3 - (a_1 a_3)' - a_2 a_2' \\ &\Rightarrow a_4 = \frac{1}{a_0}\left[\int a_3 dt - a_1 a_4 - \frac{a_2^2}{2}\right] + \frac{C_4}{a_0}\end{aligned} \tag{19}$$

$$\begin{aligned}&n \therefore (a_0 a_n)' = a_{n-1} - \frac{1}{2}\sum_{i=1}^{n-1}(a_i a_{n-i})' \\ &\Rightarrow a_n = \frac{1}{a_0}\left[\int a_{n-1} dt - a_1 a_{n-1} - .\Lambda\right] + \frac{C_n}{a_0}\end{aligned} \tag{20}$$

Note that for n=0, equation (15) doesn't provide any new solution but the same as for equations (9) and (10). Further more, considering $L(t_0) = 0$ in equations (9) and (10), results in zero values for the integration constants C_n. Next, by substituting values for a_0 from equations (15) and (16); a_n is calculated. Consequently the solution of each equations (a_n) is calculated once a_{n-1} is obtained in order.

$$a_1 = \frac{2}{3}t \tag{21}$$

$$a_2 = \left[\left(\frac{1}{2}\times\frac{2}{3}\right) - \left(\frac{1}{2}\left(\frac{2}{3}\right)^2\right)\right]\frac{t^{3/2}}{(2\lambda K_s)^{1/2}} \tag{22}$$

$$a_3 = \left[\left(\frac{2}{5}\times\frac{1}{9}\right) - \left(\frac{2}{3}\times\frac{1}{9}\right)\right]\frac{t^2}{(2\lambda K_s)} \tag{23}$$

$$a_4 = \left[\left(\frac{1}{3}\times\frac{-4}{135}\right) - \left(\frac{2}{3}\times\frac{-4}{135}\right) - \left(\frac{1}{2}\left(\frac{1}{9}\right)^2\right)\right]\frac{t^{5/2}}{(2\lambda K_s)^{3/2}} \tag{24}$$

$$a_n = \left[\left(\frac{2}{n+2}\right)k_{n-1} - \frac{1}{2}\sum_{i=1}^{n-1} k_i k_{n-i}\right]\frac{t^{n+1/2}}{(2\lambda K_s)^{n-1/2}} \tag{25}$$

Where k_n is calculated subsequently from n=1 to N as bellow

$$k_n' = \left(\frac{2}{n+2}\right)k_{n-1} - \frac{1}{2}\sum_{i=1}^{n-1} k_i k_{n-i} \qquad k_0 = 1 \tag{26}$$

Finally, by putting coefficients a_n into the equation (10), and re-transforming for parameter λ (equation (6)), the perturbation series solution of the governing equation (4) is obtained directly

$$L(t) = \sum_{i=0}^{\infty} k_n \frac{(\mu K_s)^n}{(2\alpha\mu K_s)^{n-1/2}} t^{n+1/2} \tag{27}$$

$$F(t) = n_e(1 - s_n)L(t) \tag{28}$$

Where n_e and S_n are Soil effective porosity and initial moisture; and K_n is calculated from equation (26).

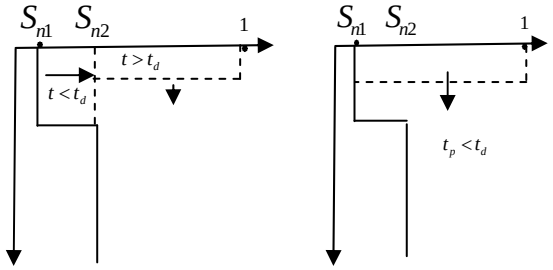

Fig. 4 occurrence of runoff after (left) and before (right) meeting moisture deficit

3.1.2 Validation and convergence

One can notice the similarity between equation (2) and the series solution, equation (27), which suggests re-writing of the series as a sum of the first two terms.

$$L(t) = \sqrt{2\alpha\mu k_s}\, t^{1/2} + \frac{2\mu k_s}{3} t + r \tag{29}$$

$$r = \mu k_s \sum_{n=0}^{\infty} k_n \left(\frac{\mu K_s}{2\alpha} \right)^{n-1/2} t^{n+1/2} \tag{30}$$

Putting equation (29) to equation (28) and comparing with Philip equation (3), defines parameters S_p and C_a as below:

$$\begin{aligned} S_p &= \left\{ 2K_s n_e (1 - s_n) \left[\phi(1) - \phi(s_n) \right] \right\}^{1/2} \\ C_a &= \frac{2}{3} K \end{aligned} \tag{31}$$

Which for dry condition ($S_n \approx 0$) reduces exactly to the corresponding parameters of Philip equation for delta-function soils, obtained by Parlange et al (1975). This implies the mathematical validation of our solution. Nevertheless, unlike the pervious work, here we obtained a simple expression for residual $R = n_e(1 - s_n)r$ which facilitates convergence criteria. Numerically, this critical time of convergence can be determined by sudden change in the sign of the few first terms of *R* series.

3.2 Non-uniform initial moisture profile

The soil evapotranspiration effect during intra-storm periods dictates the initial surface moisture S_n, which in turn affects ponding time $t_{p(Sn)}$ and total Hortonian overland flow $q_{p(Sn)}$ through following equations.

$$t_p = \frac{K_s n_e (1 - s_n) \left[\phi(1) - \phi(s_n) \right]}{q_o \left\{ q_o - K_s \left(1 - K_r(s_n) \right) \right\}} \tag{32}$$

$$q_p(s_n) = q_0 - \left\{ K(s_n) + \mu K_s n_e (1 - s_n) \left(1 + \frac{\alpha}{L} \right) \right\} \tag{33}$$

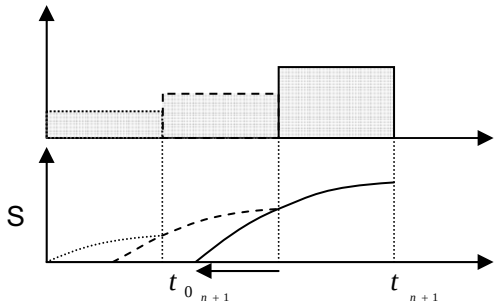

Fig. 5 formulation of continuous soil moisture growth under variable flux boundary condition

Here $q_\circ$ is the surface application rate. In most practical situations the root zone results in a step profile due to the soil moisture deficit. Traditionally, piston flow can be used after meeting moisture deficit and establishing a uniform profile at the first stage of infiltration (Fig.4, left). Nevertheless, for dry soil conditions with developed root zone, it is quite possible that ponding time occurs before establishing the uniform flow (Fig.4, right). At this condition (equation (34)) the moisture deficit approach underestimates runoff.

$$t_p(s_{n1}) \le t_d = \left(d_r n_e \left(s_{n1} - s_{n2} \right) \right) / q_0 \tag{34}$$

One simple approach can be proposed by an analytical switching mechanism between two solutions of different initial condition, so that at the critical time; the solution can switch to moisture-deficit approach (S_{n1}) with a lag time of $t_\circ$ through following set of equations.

$$L = L(s_{n1}, t) \qquad q_p = q_p(s_{n1}, t) \qquad t < t_r \tag{35}$$

$$'L = L(s_{n2}, t + t_0) \quad q_p = q_p(s_{n2}, t + t_0) \qquad t \ge t_r \tag{36}$$

where $t_\circ$ can be calculated from equations.(32), (33) and (5) as follow

$$t_0 = t_d + t_p(s_{n2}) + \frac{\alpha}{\mu K_s} \left\{ \frac{d_r - L_p}{\alpha} - Ln\left(1 + \frac{d_r - L_p}{\alpha} \right) \right\} \tag{37}$$

$$L_p = \frac{q_0 t_p(s_{n2})}{n_e (1 - s_{n2})} \tag{38}$$

3.3 Infiltration under variable flux boundary

Although it is convenient to estimate runoff under variable rainfall, but the solution of piston flow equation before runoff, assumes an essentially constant average rate at the upper boundary. One approach can be

propagation of parallel pistons for each of the rainfall pulses. Though, it may result in fast lateral growth of piston flow and estimation error in ponding time and overland flow. To avoid this, considering soil moisture at the end of a rainfall pulse (S_n), then equations (39) and (40) can be used to estimate the equivalent time to achieve the same moisture content, but under following rainfall rate n+1 (Fig. 5).Thus with correction of starting time at the beginning of each rain fall pulse, a continuous growth of surface moisture under variable rainfall can be obtained.

$$q_0 = K_s\left[K_r(s) - K_r(s_n) + \frac{n_e(s-s_n)[\phi(1)-\phi(s_n)]}{q_o t}\right]$$

$$Dt = \frac{n_e(s_n - s_i)[\phi(1)-\phi(s_i)]}{q_{n+1}\left((q_{n+1}/k_s) - K_r(s_n) + K_r(s_i)\right)} \qquad (39)$$

$$t_{0_{n+1}} = t - Dt \qquad (40)$$

3.4 Transformed analytical water budget model

Kim et all (1996) proposed analytical solutions for transient soil water budget model for inter-storm period, due to different dominant processes including only percolation (equation (41)), only evapotranspiration (equation (42)); and percolation with simultaneous evapotranspiration (equation (43)).

$$S(t) = S_0\left(1 + \frac{cK_s}{n_e d_r} S_0^{\,c} t\right)^{-1/c} \qquad (41)$$

$$S_1(t) = S_0 \exp\left(-\frac{E_p}{n_e d_r} t\right), \quad E_1 = n_e d_r S_0\left(1 - \frac{S_1(t)}{S_0}\right) \qquad (42)$$

$$S_r(t) = \left[\left(S_0^{-c} + \frac{K_s}{E_p}\right)\exp\left(\frac{cE_p}{n_e d_r} t\right) - \frac{K_s}{E_p}\right]^{-1/c} \qquad (43)$$

$$E_r(t) = n_e d_r S_0\left(1 - \frac{S_1(t)}{S_0}\right)\left(\frac{E_p}{E_p + K_s S_0^{\,c}}\right)^{1/c}$$

Where d_r and S_0 are depth of layer, and initial saturation respectively, and c is defined by $(\eta/\lambda)-1$. Now, we introduce variables A and B to transform equation (42), (43) into the simpler forms:

$$A = \left(\frac{E_p}{E_p + K_s S_0^{\,c}}\right)^{1/c}, \qquad B = \exp\left(-\frac{E_p}{n_e d_r} t\right) \qquad (44)$$

$$S_1(t) = n_e d_r S_0 (1 - B) \qquad (45)$$

$$E_1(t) = n_e d_r S_0 (1 - B)$$

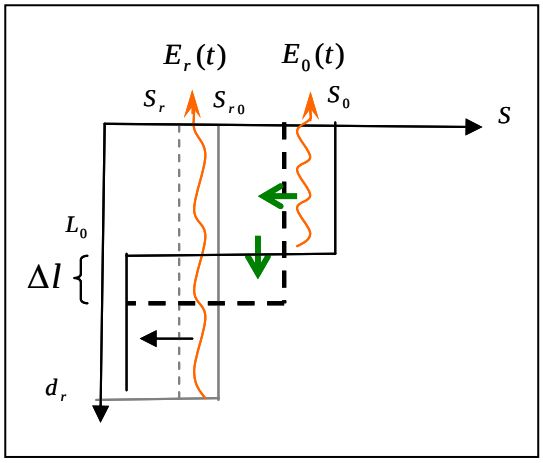

Fig. 6 Effect of root zone in the early stage of redistribution

$$S_r(t) = S_0 A (A^c + B^{-c} - 1)^{-1/c} \qquad (46)$$

$$E_r(t) = n_e d_r S_0 A (1 - B)$$

These simpler forms facilitate coupling Kim's analytical water budget model into the proposed piston flow to estimate simultaneous recharge and evapotranspiration at this report.

3.5 Redistribution under soil evapotranspiration

At the first stage of redistribution, wetting front might be within evapotranspiration depth (d_r) which can be much deeper than common root zone values. Bazie et al (1995) measured this depth up to 2.5 m through a 7-meter lysimeter under their experimental condition. As a result the lumped water budget approach for such layer can't predict the travel time of wetting front and can be misleading in prediction of surface soil moisture. Hence developing an equivalent wetting front under simultaneous evapotranspiration and percolation was considered.

Equivalent wetting front: Considering wetting front at time t as an arbitrary layer with depth and saturation ratio of L_0 and S_0, one can imagine the propagation of the wetting front (Δl) over time span Δt, as a result of percolation from this arbitrary layer as depicted in Fig.6 Due to slow motion of the wetting front in redistribution phase, the error can be acceptable if we choose Δt

values small enough. Accordingly, the transient water budget can be written as below.

$$\Delta l.n_e\left[s(\Delta t)-s_n\right]=q_p(\Delta t)-E_f(\Delta t) \qquad (47)$$

$$q_p(\Delta t)=.n_eL_0\left[s_0-s(\Delta t)\right]-E_0(\Delta t) \qquad (48)$$

Where n_e is effective porosity, and evapotranspiration at wetting front (E_f) is estimated from corresponding values for the arbitrary layer (E_0) and the lumped root-zone layer (E_r).

$$E_f(\Delta t)=E_r(\Delta t)-E_0(\Delta t) \qquad (49)$$

Equation (49) is quite a practical assumption that not only facilitates calculation of Δl but also can considers variable-depth evapotranspiration for further applications

$$\Delta l=\frac{n_eL_0\left[s_0-s(\Delta t)\right]-E_r(\Delta t)}{n_e\left[s(\Delta t)-s_n\right]} \qquad (50)$$

$$L(\Delta t)=L_0+\Delta l$$

Where the variables on the right hand side can be estimated by the transformed water budget equations

$$S(\Delta t)=S_r(\Delta t)=S_0A(A^c+B^{-c}-1)^{-1/c},\ d_r=L_0 \qquad (51)$$

$$E_r(t)=n_ed_rS_{r0}(1-B) \quad , \quad S_{r0}=\frac{L_0}{d_r}S_0 \qquad (52)$$

Substituting equation (52) into (50) and then into (47) gives the equivalent wetting front due to simultaneous evapotranspiration and percolation at small time span of Δt :

$$L(\Delta t)=\left(\frac{S_0B-S_n}{S(\Delta t)-S_n}\right) \qquad (53)$$

Which for initial dry condition [$S_n=0$] can be simplified as below

$$L(\Delta t)=\left\{\frac{B_r}{A}(A^c+B^{-c}-1)^{-1/c}\right\}L_0 \qquad (54)$$

Thus considering travel time of $n\Delta t$, equivalent front depth at any time step can be estimated based on the front depth at the last time step as the updated L_0 value.

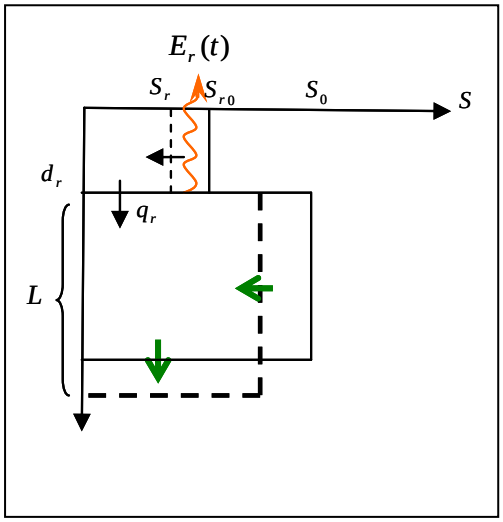

Fig.7 Effect of root zone in the late stage of redistribution

3.6 Redistribution under flux boundary

In the later stage of redistribution, when the wetting front is passing down the depth (dr), the transformed water budget equations can be applied for prediction of evapotranspiration and simultaneous percolation to the lower layer (Fig. 7). That necessitates introducing of a leakage factor q_r for boundary condition in the depth averaged continuity equation.

$$q_r-K(s_n)=\frac{d}{dt}\left[n_eL(S-S_n)\right] \qquad (55)$$

Which, with deviation due to t and integration from t=0 to t, results in equations (56) and.(57) respectively

$$q_r-K(s_n)=n_e(S-S_n)\frac{dL}{dt}+n_eL\frac{ds}{dt} \qquad (56)$$

$$Q-K(s_n)t=n_eL(S-S_n)+n_eL_0(S_0-S_n)=n_eL(S-S_n)-V_0 \qquad (57)$$

In which leakage terms q_r and Q are calculated from the transformed water budget equations for Upper layer as below

$$q_r=K(s_r) \qquad (58)$$

$$Q=n_ed_r\left[s_0-s_r(t)\right]-E(t)=n_ed_rS_0\left\{1-A\left[(A^c+B^{-c}-1)^{-1/c}+(1-B)\right]\right\}$$

Consequently the depth averaged Darcy law can be stated in terms of stream tube formulation and flux potential as equations (60) and (61) respectively

$$\bar{q} = n_e(S - S_n)\frac{dL}{dt} + K(s_n) \quad (60)$$

$$\bar{q} = K(s) + \frac{\phi(s) - \phi(s_n)}{L} \quad (61)$$

That is

$$n_e(S - S_n)\frac{dL}{dt} = K(s) - K(s_n) + \frac{\phi(s) - \phi(s_n)}{L} \quad (62)$$

Putting equation (62) into (56) and re-arranging in terms of S, leads to general derivative equation (63)

$$\frac{ds}{dt} = -\frac{K_s}{n_e L}\left[s^{\eta/\lambda} + \left(\frac{\psi_b}{1-\eta}\right)\left(\frac{s^{\eta-1/\lambda} - s_n^{\eta-1/\lambda}}{L}\right) - \frac{q_r(t)}{K_s}\right] \quad (63)$$

$$L = V_0 + \frac{[Q(t) - K(s_n)t]}{n_e(s - s_n)} \quad (64)$$

This facilitates solution of equation (63) by Runge-Kutta 4th order numerical integration.

Validation: One can notice that equation (63) is not a completely new form, but a general formula which can be reduced to more restricted solutions of Dagan-Bressler (1981), or the one by Ogden and Saghafian (1997) for redistribution due to depletion in rainfall rate below the saturated permeability (r<Ks in Table 3).

3.7 Formulation for kinematic wave

In many cases it is quite convenient to apply 1-D kinematic wave model, considering eight directions from each node to the others. Though, this needs that the dimensions of cells to be considered small enough, otherwise the derivation of the actual overland flow from those main directions may lead to high errors in large distances. As a solution, Liu et al (2004) applied isoparametric formulation of 2-D finite difference grids to provide 1-D kinematic wave equation in all directions. Nevertheless, they used an explicit finite difference volume formulation. Here the explicit and implicit scheme was developed (equation (65) to (68)).

a) The explicit estimator

$$q_{i,j}^{k+1} = \frac{\frac{\Delta t}{\Delta\bar{x}\Delta\bar{y}}\left[(q_x\Delta y)_{in} + (q_y\Delta x)_{in}\right] + \alpha\beta\, q_{i,j}^{k}\left[(q_{i,j}^{k} + \bar{q}_{in})/2\right] + R}{\frac{\Delta t}{\Delta\bar{x}\Delta\bar{y}}\left(\cos\gamma.\Delta y_{i\pm\frac{1}{2},j} + \sin\gamma.\Delta x_{i,j\pm\frac{1}{2}}\right) + \alpha\beta\left[(q_{i,j}^{k} + \bar{q}_{in})/2\right]^{\beta-1}} \quad (65)$$

$$R = \Delta t\left[(r_{i,j}^{k} + r_{i,j}^{k+1})/2\right]$$

b) The implicit corrector

$$C = \alpha\left(q_{i,j}^{k}\right)^{\beta}\frac{\Delta t}{\Delta\bar{x}\Delta\bar{y}}\left[(q_x\Delta y)_{in} + (q_y\Delta x)_{in}\right] + \Delta t\left[(r_{i,j}^{k} + r_{i,j}^{k+1})/2\right] \quad (66)$$

$$f\left(q_{i,j}^{k+1}\right) = \alpha\left(q_{i,j}^{k+1}\right)^{\beta} + \frac{\Delta t}{\Delta\bar{x}\Delta\bar{y}}\left(\cos\gamma.\Delta y_{i\pm\frac{1}{2},j} + \sin\gamma.\Delta x_{i,j\pm\frac{1}{2}}\right)q_{i,j}^{k+1} - C \quad (67)$$

$$f'\left(q_{i,j}^{k+1}\right) = \alpha\beta\left(q_{i,j}^{k+1}\right)^{\beta-1} + \frac{\Delta t}{\Delta\bar{x}\Delta\bar{y}}\left(\cos\gamma.\Delta y_{i\pm\frac{1}{2},j} + \sin\gamma.\Delta x_{i,j\pm\frac{1}{2}}\right) \quad (68)$$

Where, α, β and q are kinematic wave parameters.

4. Verification

Regarding analytical framework of the proposed equations, they don't need validation as needed for numerical methods. However, here the application of proposed equivalent series for a soil column is examined, and then the other developed equations were integrated and verified for an assumed quadratic basin.

Table 3 global parameters for generalized redistribution equation

	Case of Etp = 0 (Dagan-Bresler)	Case of (r <Ks) (Ogden, 1997)	Case of Etp ≠ 0 (proposed)
d_r	0	0	d_r
$q_r(t)$	0	Parameter in equation (63)	Eq.(58)
Q	0	$r(t - t_0)$	Eq.(59)

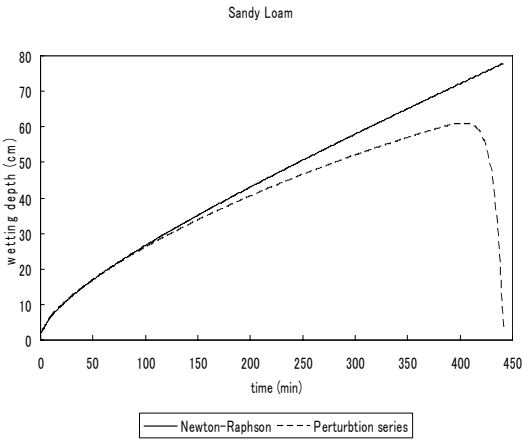

Fig. 8 equivalent series solution compared to piston flow for a sandy loam under a rainfall rate of 9cm/hr

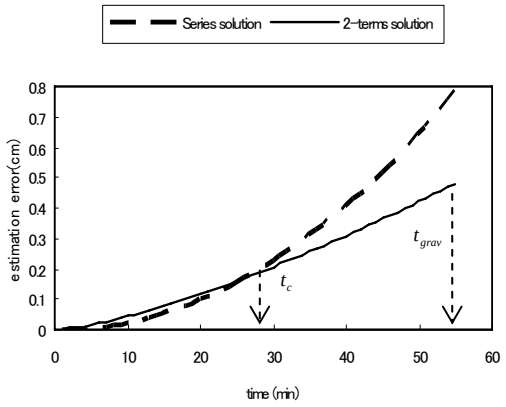

Fig. 9 Truncation estimation error for a Sandy loam

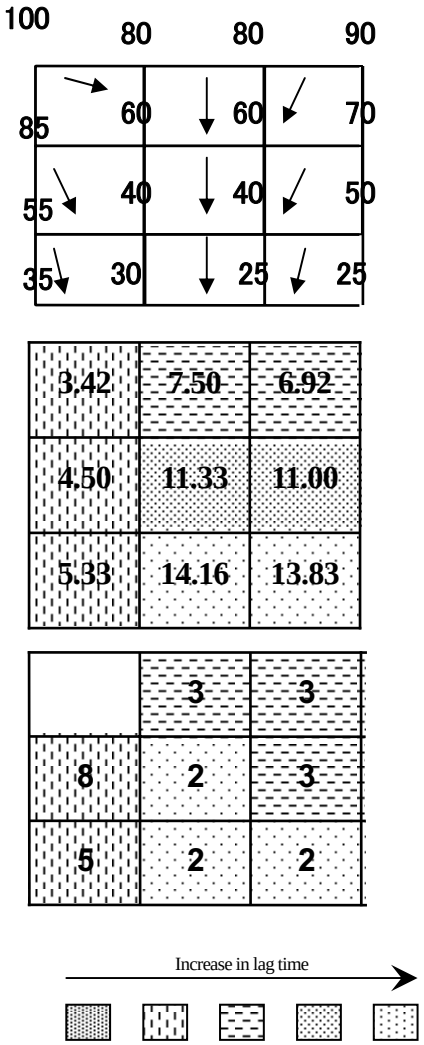

Fig.10 patterns in recharge lag time in days (below) and runoff period in hrs (middle) compared to topography)

4.1 Equivalent series for piston flow

Fig.8 compares simulation results by equivalent series with one by piston flow. It shows a good adaptation before critical time when the residual series (equation (30)) converges. Hence, considering piston flow as the analytical solution for delta function soils, the estimation error of series solutions can be estimated. This error has been simulated and compared for full series (n=100 in equation (27)), and truncated one (n=0, 1) in Fig. 9. As it can be expected, the estimated convergence time (t_c) marks the point where the residual series gains negative values and tends to infinity. That's quite physically sensible. Further, it reveals that for delta-function soils, the convergence domain of series R(n=100) ($t < t_c$) is smaller than the experimental characteristic time (t_{grav}) suggested by Philip (1969)

4.2 Coupling mechanism

Despite the convenience of analytical solutions, they can hardly handle complex situations such as simultaneous evapotranspiration, infiltration, percolation, volume and lag time of table recharge. As a key approach to integrate all these processes, this study formulates a two-front piston flow approach within a water budget framework as the coupling mechanism (Fig. 2). Thus once the deeper wetting front reaches the water table, it incorporates into water budget model for recharge, the upper front will start percolation independent of surface processes, and a new (shallow) front will be developed after the first coming infiltration

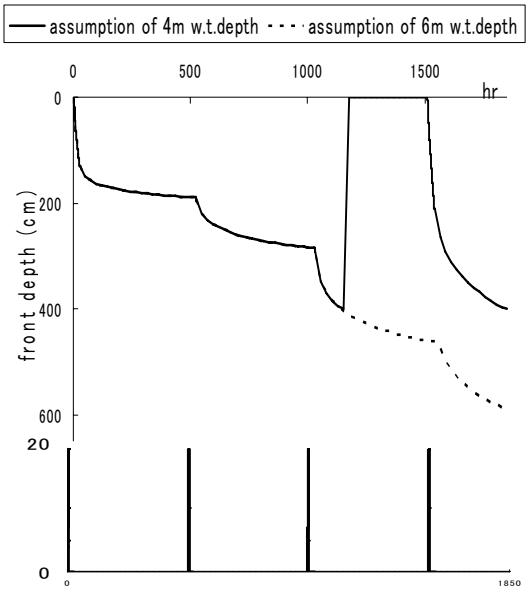

Fig.11 Comparing travel time of wetting front with assumptions of water table depth of 6m, and 4m under same rainfall (max 19.08mm) and soil condition.

events. Nevertheless any effective coupling mechanism should carry "feed back" effect of the processes as well. Note that here, for the sake of a complete coupling mechanism the kinematic wave equations were involved through a conceptual quadratic basin instead of single soil columns (Fig.10).

4.2.1 Effect of runoff on recharge

As mentioned before, prediction of two-dimensional recharge patterns (recharge rate, and delay time) combined with aquifer transmissibility can be used as weighting factors to allocate the "sustainable yield" of aquifer to pumping well fields. Due to the significance of such patterns in conjunctive use, the capability of the proposed model was verified through the simulation

depicted in Fig10. Thus for same soil and rainfall conditions, the obtained pattern reveals a good correlation with overland flow duration which in turn is affected by topographic conditions and two-dimensional patterns of lag time in water table recharge.

4.2.2 Effect of recharge on Runoff

In a water budget framework, one can expect that for the same rainfall events the higher water table results in

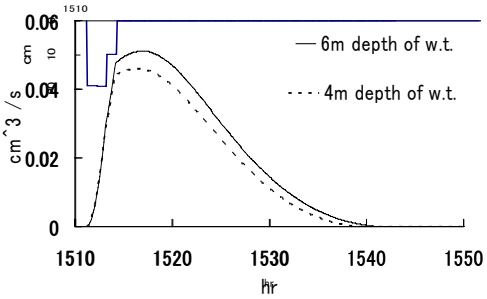

Fig.12 Effect on water table depth on overland flow, after arrival the first wetting front to the assumed w.t. of 4m (t=1000hr)

higher soil moisture and consequent excess-infiltration overland flow. Although in more realistic profile modeling, it can't happen until the wetting front reaches the water table. This travel time for a water table depth of 4m was simulated and compared with the corresponding time for 6m depth of water table (Fig.11). Hence, the following rainfall event results in a new wetting front, while at the assumed thicker vadose zone (6m), the existing wetting front continue percolation. This results in higher surface soil moisture and the consequent overland flow for the former one as simulated in Fig.12**.**

5. Regional application

The capability of the proposed methodology needs to be examined within a distributed modeling system under typical conditions that "aquifers mining" might happen. Such conditions are more common in arid regions where there are not permanent rivers with acceptable water quality. Consequently, while the coarser deposits at the base of mountainous boundaries trap historical floods and subsurface inflow; the fine-grain deposits with transmissibility and saline water define the lower boundary conditions.

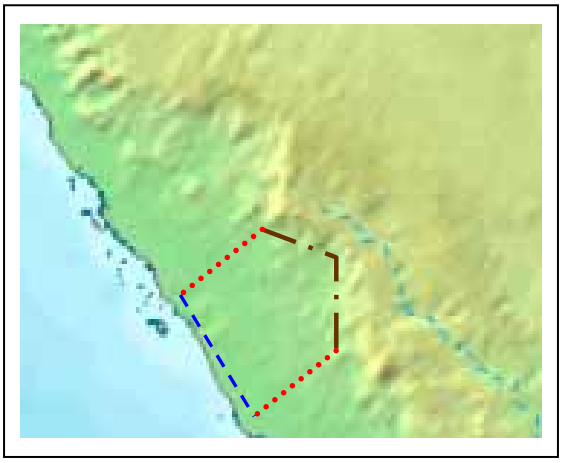

Fig. 13 Typical boundary conditions at the western coast of Saudi Arabia: (no-flow boundaries are doted)

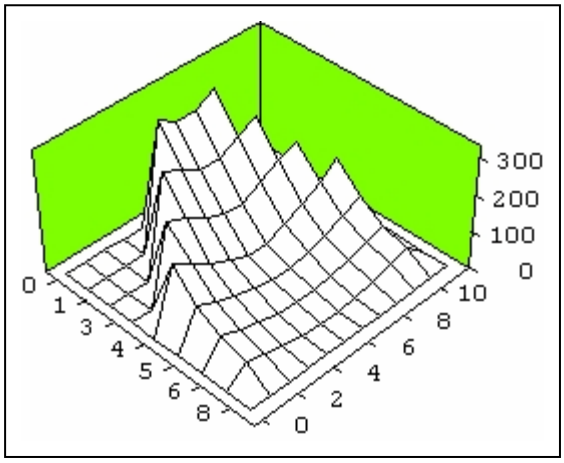

Fig. 14 topography and slope directions for isoparametric kinematic wave model.

5.1. Typical parameters and boundaries

The typical boundary conditions are described for an example in the western coasts of Saudi Arabia in Fig.13; where deep aquifers are the important water resources, and long term recharge needs to be analyzed through one-dimensional solution of Richard equation. Although, for the sake of exploring the concept of "dynamic storage" of the system as proposed by this study, a typical topographical condition (Fig. 14) and a set of model parameters with mesh size of 2km was assumed (Fig. 15) and then the surface and subsurface components of inflow were simulated for a generic scenario of periodical rainfall-evapotranspiration condition.

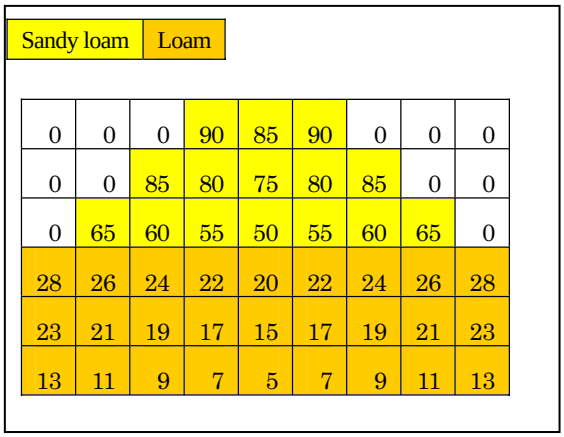

Fig. 15 distribution of soil type and water table depth over the model cells

5.2. Temporal availability of inflow

A conjunctive-use scheme has to consider the availability of dynamic storage of surface and subsurface resources in different time span. To achieve this, here assumed that a potential dam site at downstream cell can be considered so that it can prevent discharging floods to the salty water body (sea) downhill. Now, by comparing the pulses of inflow to the reservoir (runoff) and the aquifer (recharge), an approximate allocation rule between surface and ground water resources can be obtained. Though to obtain detailed rules they need to be combined with temporal changes in aquifer transmissibility as well. Note that in Fig.16 even though, disperse and low rainfall rate in dry seasons can't produce significant runoff, but they can contribute to aquifer recharge, make them the dominant water resources in arid regions

5.3. Spatial availability of recharge

As mentioned before, the spatial allocation of safe yield from different groundwater model cells (well fields) can be weighted by aerial recharge and net lateral inflow to each model cell/zone. This implies the significance of spatial distribution of aerial recharge as well as lag time in recharge. Fig.17 compares these two parameters at two different model cells with water table depth of 5 and 50 meter respectively. Accordingly, while shallow water table condition reveals sharp pulses of recharge, the recharge pulses at deeper aquifer tends to merged into few delayed pulses at deeper water table. This implies the heterogeneity in aerial recharge that can be used as a key toward spatial and temporal well regulation in conjunctive use management.

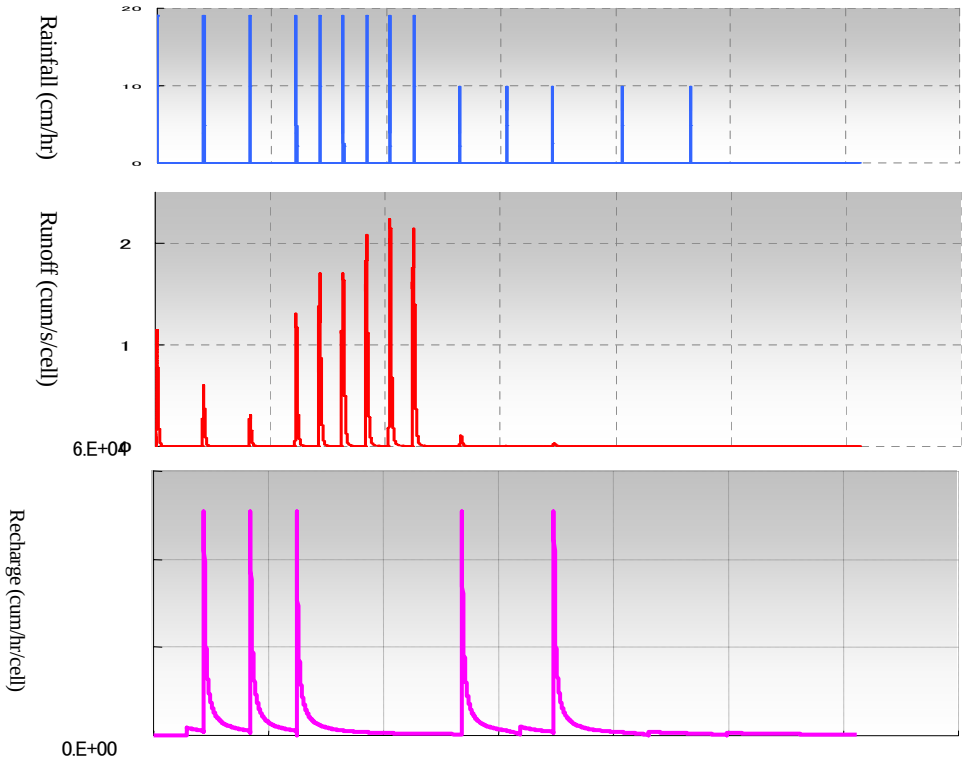

Fig. 16 shallow water table recharge (bottom) and inflow (cum/5min) at potential dam site (middle) for periodical rainfall-evapotranspiration (above)

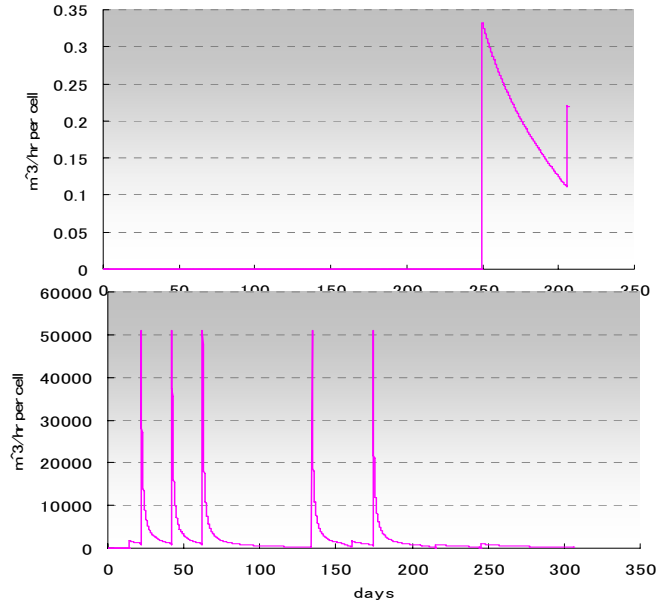

Fig. 17 recharge pulses at 5m (down) and 50 m (up) water table depth.

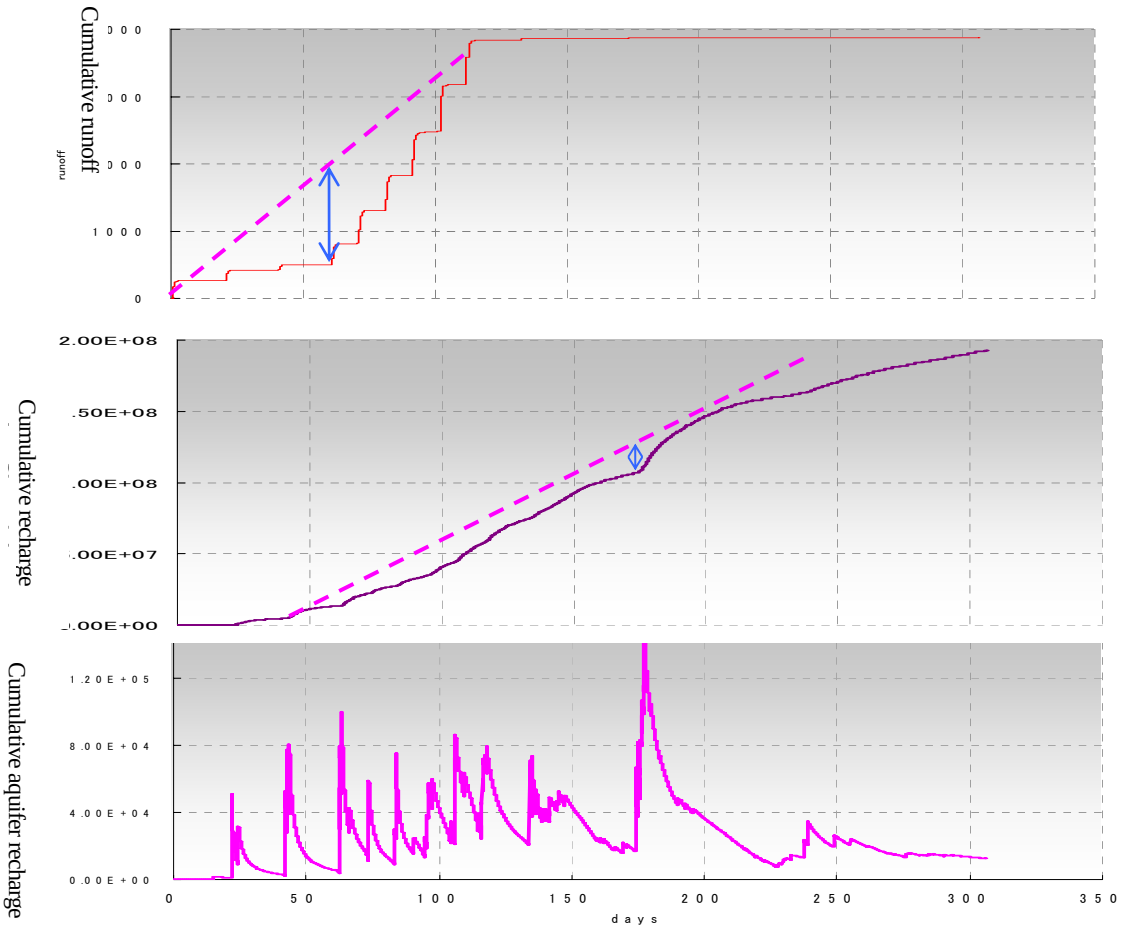

Fig. 18 total aquifer recharge (down) and mass curve analysis of the net recharge compared with inflow mass curve analysis into potential dam site

5.4. Primary allocation rules

As one can expect the pick recharge of aquifer must have a lag time compared to the reservoir pick inflow. This is mainly due to the retarding mechanism of unsaturated zone which is heterogeneous in terms of thickness and soil hydraulic parameters. As a result, even the lumped estimation of the aquifer recharge and lag time has to be simulated as the summation of calculated recharge within a distributed system. This is what has been done in Fig.18. As it can be seen, the resultant pattern doesn't correlate with individual patterns in each cell, but can be sought of weighted average of model cells. Hence, for each time period depends of distribution of water table recharge a set of primary allocation coefficients can be provided.

5.5. Lumped upper and lower rules

Shortly, the proposed primary rules try to allocate a "permissible" withdrawal from different pumping wells and in different time periods. Now, the question that arises is how to decide these permissible values. That needs to be analyzed within boarder domain of conjunctive use of surface and ground water resources. Again here we take the benefit of our methodology which facilitates generating recharge long time series, which in turn enables us to expand "mass curve analysis" techniques for conjunctive use operation as following.

Upper rules: assuming the initial water table depth at the minimum recharge conditions, the tangents (Fig.18) define the average demand which can guarantee a minimum storage. This minimum water level (due to average permissible withdrawal) is highly dependent on return period for maximum probable inflow/recharge events. For example, considering longer analysis, as shown in Fig.19 suggests a more realistic estimation.

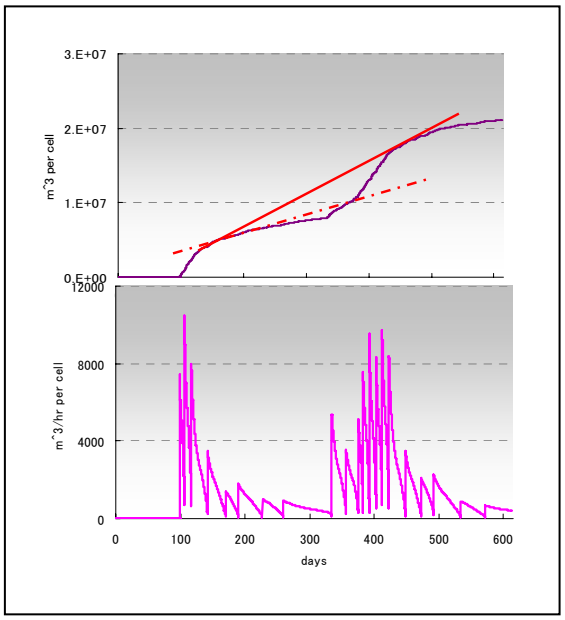

Fig. 19 mass curve analysis (above) of aquifer recharge (down) for longer time period

Lower rules: for large recharge events within every 10-15 years, an effective conjunctive use should consider minimum withdrawal to trap the events into the storage. From this point of view, the average withdrawal rate depicted as dot line in Fig.19 can't be an effective policy to trap the following recharge event for average depth of water table. Another strategy can be utilizing the inflow at the downstream cell for artificial recharge of the aquifer. Yet, if the arrival time of resulting recharge pulses coincides with the corresponding time for a large event, then it may overflows to sea and makes all the costs of recharge facilities in vein.

6. Discussion

This report as the first output of the research program has to consider further development of the obtained results both in modeling and management aspects.

6.1. Continuity in overland flow

The infiltration rates that are calculated implicitly as the result of profile modeling (wetting front) are more physically sensible and reliable for infiltration-excess (Hortonian) overland flow. Though, for area where the horizontal component of subsurface flow (interflow) is not ignorable, it can be misleading. This happens especially at mountainous basins with gaining streams where discontinuity in hydro-geologic setting can be

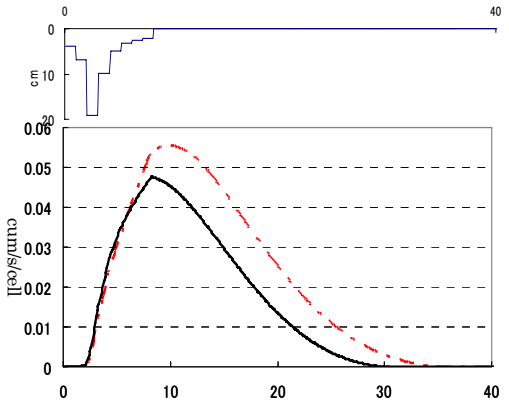

Fig.20 correlation of overland flow by piston flow equation (solid curve) and by equivalent series (dashed)

simplified by subsurface linear storage models rather than three dimensional solutions of Richard equation. As an approach, an explicit surface infiltration formula linked with serial linear storages can be applied to such sub-area of conjunctive use domain. Nevertheless, the overland flow that discharges from mountainous basin over the plain area might have a discontinuity due to the different infiltration calculation at these areas because of different between infiltration parameters. That's why at this research the equivalent explicit series for Piston flow was proposed to guarantee a uniform infiltration process over the whole domain with different subsurface conditions. Fig. 20 compares the hydrograph generated by these two approaches. As it can be seen difference between two methods are not significant and can be adjusted by calibration for the depth of surface layer. Note that the equivalent series was applied within "Time Compression Approximation" (TCA) method (Kim et al, 1996) to calculate pounding time with accuracy.

6.2. Sensitivity to soil moisture distribution

Another important issue in deriving long recharge time series, is that how the assumed uniform initial f soil moisture can affects the simulation results. The simulated soil moisture distribution (Fig. 21) in the assumed basin reveals that even by assuming a uniform moisture condition of 0.1, a heterogeneous soil moisture distribution can be obtained after a few rainfall events. Yet, the redistribution phase decreases such heterogeneity significantly, making the initial condition more uniform. This verifies the convenient assumption of uniform initial moisture at the end of a dry season as the initial condition before applying historical data.

0.00000	0.00000	0.00000	0.70381	0.71655	0.71385	0.00000	0.00000	0.00000
0.00000	0.00000	0.70440	0.71385	0.73988	0.73899	0.71451	0.00000	0.00000
0.00000	0.70500	0.71933	0.73061	0.79352	0.79671	0.75219	0.71586	0.00000
0.81290	0.83510	0.87165	0.91089	1.00000	1.00000	1.00000	0.99032	0.84279
0.83808	0.88826	0.95026	1.00000	1.00000	1.00000	1.00000	1.00000	1.00000
0.85983	0.90906	1.00000	1.00000	1.00000	1.00000	1.00000	1.00000	1.00000

0.00000	0.00000	0.00000	0.41013	0.41059	0.41049	0.00000	0.00000	0.00000
0.00000	0.00000	0.40988	0.41053	0.41137	0.41131	0.41021	0.00000	0.00000
0.00000	0.40990	0.41053	0.41090	0.41215	0.41219	0.41141	0.41025	0.00000
0.53147	0.53236	0.53296	0.53352	0.53855	0.53869	0.53663	0.53470	0.53256
0.53214	0.53327	0.53390	0.53459	0.54279	0.54355	0.54250	0.53927	0.53473
0.53267	0.53349	0.53419	0.53513	0.55395	0.55118	0.55018	0.54532	0.53927

Fig.21 distribution of surface soil moisture by assuming uniform initial saturation of 0.1, after a few rainfall events (up) and after the following evapotranspiration period (down)

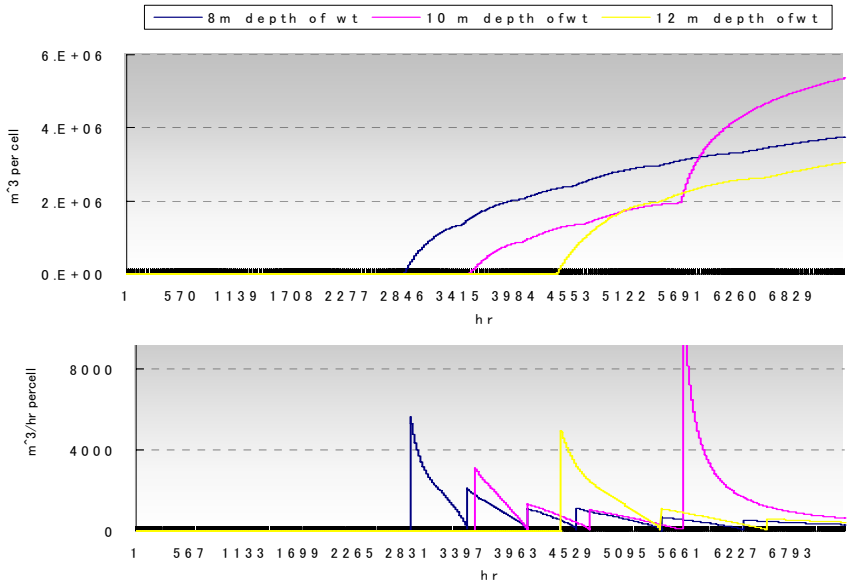

Fig.22 Non-linearity in shallow water table recharge at 8m, 10m and 12 m of water table depth

6.3. Non-linearity in Water table recharge

One of the main concerns in models that simulate vadose zone and aquifer separately is how to estimate recharge at the water table. The problem arises because the estimation of recharge depends on the depth of water table, which in turn has to be calculated by assuming recharge. As a solution, many of such models consider linear condition for recharge that facilitates later inter/extrapolation. Though, comparing simulated recharge at three different shallow depths (Fig.22) implies significant nonlinearity in recharge-depth relationship at shallow water tables. In other words, under such condition (shallow depth) the ground water

model needs to be coupled rather than just "linking the results" as assumed in "safe yield" proposed at this study. Though, for deeper water table due to tendency of wetting front to merging each other, the assumption of linearity in recharge still can be considered

6.4. Toward more practical allocation rules

The proposed "primary allocation coefficients" tries to distribute a lumped permissible withdrawal to different model cells only based on water table recharge patterns, ignoring the lateral recharge from adjacent cells in the aquifer. Hence in the next step of this research, the primary coefficients have to combine with aquifer transmissibility (T) in such a way that guarantee a sustainable yield from each model cells (well fields) in different time span (stress period). Such "temporary allocation coefficients" can be provided for decision makers in terms of tables for a few months ahead. Thus they need to be simulated for new input data.

Another approach which is more approximate but attractive to decision makers, can be sought of "average allocation coefficients" for different hydro-climate and depth of water table conditions, without the need for repeating modeling procedure in future. This can be achieved by analyzing the generated historical time series of water table recharge components to obtain average coefficients for different recharge and water table depth conditions. Thus, the only updating task would be measuring the depth of water table and calculating transmissibility components for each month.

6.5. Sustainability of conjunctive use

In the proposed "mass curve analysis technique" the longer period we consider, the larger recharge can be trapped and consequently the higher demands can be met. Though one question that arises, would be how long the renewable period can be assumed. This can be answered through principle of sustainability for conjunctive use as proposed here

1) The natural resources should pass through generation in a renewable manner (social sustainability). Hence, the "renewable period" in mass curve analysis shouldn't exceed each generation "growing period".

2) The estimated minimum level under such "permissible withdrawal" shouldn't result in irreversible environmental impacts (environmental sustainability). In other words, the major environmental threat such as soil salinity, aquifer pollution and potential sustainability need to be simulated to impose secondary constraints on permissible withdrawal and allocation rules as the further steps of this research.

Note that analyzing pumping and facilities costs in conjunctive use (economic sustainability) has been considered by many researches and is not going to be discussed at this research proposal.

7. Conclusion

An analytical approach was formulated, verified and applied for estimating permissible yield for conjunctive use, based on generating historical recharge time series for more realistic initial and boundary conditions in conjunctive use application. Though, the proposed operation rules including upper, lower and primary allocation rules, need to be re-edited by imposing secondary environmental constraints simulated by root zone salinity and solute transport model as the further steps of this research.

References

Bazie P., B. Dieng and P. Ackerer (1995): Water balance in unsaturated soil under Sundo-Sahelian climate, Estimate of the Groundwater Recharge. Rev. Sci. Eau. 8(2).

Chen, Z. Q., R.S. Govindarju, and L.M. Kavvas (1994): Spatial averaging of unsaturated flow equations under infiltration condition over arealy averaged heterogeneous field, Water Resour. Res. 30, 523-533.

Courant R. and D. Hilbert (1989): Methods of mathematical Physics, Wiley-interscience.

Dagan,G., and E. Bresler (1981): Unsaturated flow in spatially field , Water Resour. Res. 19(2).

Kim C. P., J.N.M. Stricker, and P.J.F.Torfs (1996): An analytical framework for the water budget of the unsaturated zone, Water Resour. Res. 32(12).

Liu, Q.Q., L. Chen and V.P. Singh (2004): Two-dimensional Kinematic wave model of overland-flow, J. Hydrol 291 28-41.

Ogden, F. and B. Saghafian (1997): Green-Ampt infiltration with redistribution, Journal of irrigation and Drainage Eng. September/October 1997, 386-393.

Parlange, J,Y. (1975): On the flow in unsaturated soils by optimization. Soil Sci. of Am. Proc., 1975,5, 415-418.

Philip, J.R. (1957): The theory of infiltration: the infiltration equation and its solution. Soil Sci. 83.

Philip, J.R (1969): Theory of infiltration. Adv. Hydrosci. 5*215-296.

Salvucci, G.D., and D.Entekhabi (1994): Explicit expression for Green-Ampt infiltration rate and cumulative storage, Water Resour. Res., 30*2661-2663.

Sharma, M.L., G.L.Mullen and R.J. Luxmoore (1979): Soil spatial variability and its consequences on simulated water balance. Ware Resour. Res.15

水収支を考慮した表面流と地下浸透流の有機的結合シミュレーション

Sina NASOUHI*・浜口俊雄・小尻利治

*京都大学大学院工学研究科

要　旨

表流水・地下水資源の有機的結合利用によって，長時間流入を解析すれば「帯水層採掘」は上下流の集中型操作ルールを純揚水量に適用せずにすむ。これを実現する数式展開を提案し，ピストン流の浸透式に一層自然な初期条件を組み込んだ。これは，キネマティックウェーブ・地下水涵養の解析水収支両モデルを連成した2ピストン構造を考察するのに役立つ。本提案手法はまず土柱に対して検証した後，よくある乾燥地帯の条件に適用した。

キーワード：有機的結合利用，操作ルール，ピストン流，キネマティックウェーブ，解析水収支，地下水涵養，摂動理論